Available online at www.sciencedirect.com

ScienceDirect

journal homepage: www.elsevier.com/locate/he

Partial inhibition of the inter-photosystem electron transfer at cytochrome b_6f complex promotes periodic surges of hydrogen evolution in *Chlamydomonas reinhardtii*

Fatemeh Khosravitabar, Fikret Mamedov *

Molecular Biomimetics, Department of Chemistry – Ångström Laboratory, Uppsala University, Box 523, Uppsala, 751 20, Sweden

HIGHLIGHTS

- Photosynthetic electron transport can be tuned for H_2 production in Chlamydomonas.
- It was achieved by partial inhibition of the Cytochrome b_6f complex.
- DNP-NT and DBMIB inhibitors were used at suboptimal concentrations.
- This results in extended H_2 production for 15 and 30 days respectively.
- Periodic surges with high rates of H_2 evolution were also detected.

GRAPHICAL ABSTRACT

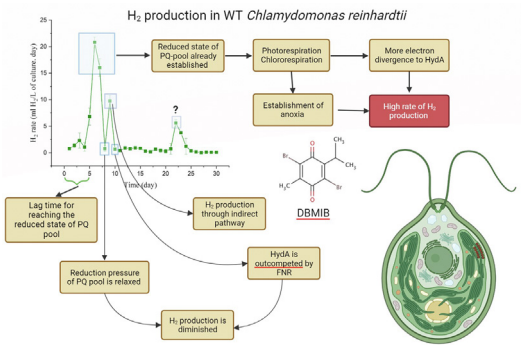

ARTICLE INFO

Article history:
Received 6 February 2023
Received in revised form
7 May 2023
Accepted 5 June 2023
Available online 20 June 2023

Keywords:
H_2 production
Chlamydomonas reinhardtii
Cytochrome b_6f
DBMIB
DNP-NT

ABSTRACT

Periodic surges of H_2 evolution were observed in the wild-type strain CC-5325 of the green unicellular alga *Chlamydomonas reinhardtii* in the presence of the electron transport inhibitors dibromo-6-isopropyl-3-methyl-1,4-benzoquinone (DBMIB, 3.5 μM) and 2,4-dinitrophenylether and iodonitrothymol (DNP-INT, 0.6 μM). Addition of DBMIB partly inhibited the electron transfer from Cytochrome b_6f complex to Photosystem I, over-reduced the plastoquinone pool, gradually inhibited photosystem II and created anoxic conditions in cells. During 30 days of anaerobic incubation, continues H_2 photoproduction with a minimum rate of 1 ml/L of culture per day was accompanied with additional outbursts of H_2 evolution. The first noticeable peak of H_2 evolution was observed on day 6 of incubation, with maximum rate of 23 ml of H_2 per L of culture per day. It was repeated on day 9 and day 22 with the 2 and 4 times lower rates respectively. Addition of DNP-NT showed similar effect by inducing the H_2 photoproduction for 15 days, albeit at much lower rates. Contribution of the direct and indirect pathways to the H_2 production is shown

* *Corresponding author.*
E-mail address: fikret.mamedov@kemi.uu.se (F. Mamedov).

https://doi.org/10.1016/j.ijhydene.2023.06.050

by fluorescence, thermoluminescence and electron paramagnetic resonance spectroscopy. It is proposed that photosynthetic electron transport in combination with photorespiration, chlororespiration and starch accumulation can switch on and off between photosynthetic, H_2 producing and survival modes of cell metabolism. Controlled switching between these modes could potentially maintain the long lasting photosynthetic H_2 production in the wild-type of Chlamydomonas.

Introduction

Molecular hydrogen (H_2) stands out as a unique energy carrier. It is known as an efficient and the clean fuel with great potential contribution to the future sustainable energy landscape [1]. Biological H_2 photoproduction using green microalgae could be an integral part of this contribution [2–4]. Green unicellular photosynthetic algae such as *Chlamydomonas reinhardtii* retained capacity to photoproduce H_2 at certain environmental conditions. This process is catalyzed by fast turnover Fe–Fe hydrogenase (HydA) which is directly coupled to the light-driven photosynthetic reactions [5,6].

Oxygenic photosynthesis to which all green algae belong, is driven by two photosystems, Photosystem II (PSII) and PSI (Fig. 1). PSII uses absorbed photons to initiate the electron transfer along the thylakoid membrane by extracting electrons from water and by reducing the plastoquinone (PQ) pool [7]. The redox reactions are continued at the cytochrome (Cyt) b_6f complex which acts as a redox intermediator between PSII and PSI [8]. PSI further energizes electron transfer by using energy of absorbed photon to reduce small soluble stromal protein ferredoxin (Fd) [9]. Photosynthetic electron transfer chain (PETC) is accompanied with the increase of proton (H^+) concentration across the thylakoid membrane in the lumen by reactions in PSII and Q-cycle in Cyt b_6f complex [10].

The fate of electron from Fd is determined by how cells behave under changing environmental conditions. Electron delivery to Calvin-Benson-Bassham (CCB) cycle through the ferredoxin $NADP^+$ oxidoreductase (FNR) and $NADP^+$ reduction completes the linear electron transfer which is the major pathway for carbon assimilation and sustaining the life cycle [11]. Some Fd electrons are diverted to the cyclic electron flow driven by PSI which could be quite high in Chlamydomonas [12,13]. At certain over-reduced conditions, such as anaerobiosis, the electron pressure in the thylakoid membranes can be relieved by diverting electrons from Fd to HydA and production of molecular H_2 (Fig. 1).

Production of H_2 by HydA is light-driven by PSI through two distinct pathways. In the direct pathway, electrons are delivered from the water splitting activity of PSII. In the indirect pathway, electrons are supplied from the degradation of carbohydrates and also delivered to the PQ-pool in the thylakoid membrane (Fig. 1) [4,14–17]. The direct pathway is the most attractive for implementation in renewable energy projects since it has least energy losses during the H_2 generation and uses water as an electron source.

In the nature, however, H_2 photoproduction in Chlamydomonas is transient and ceases within a few minutes of illumination. There are two reasons for this. Once the electron transport is fully operational under illumination, electron transfer to HydA is outcompeted by the reduction of FNR, thus directing electron flow toward the CCB cycle [18]. And subsequently, O_2 produced by PSII irreversibly inactivates HydA [19,20]. The inferior competitiveness of HydA with NADPH production, and the O_2 sensitivity are two main obstacles for sustainable microalgal H_2 photoproduction.

In Chlamydomonas which is used as a model organism for H_2 production these obstacles can be at least partially overcame by down-regulation of the PSII activity either by nutrient deprivation [16,20–26] or mutagenic approach [17,27–29]. Although some robust mutants, such as pgr5 {Steinbeck, 2015 #54} or hpm91 [30], in combination with certain upgrading strategies like addition of safe O_2 scavengers to media culture [31,32] or enhanced chloroplast-mitochondria crosstalk [33] have improved H_2 production to some extent, the maximum light to H_2 conversion efficiency is still far from the theoretically desirable yield of 13% [4]. Commercial viability of large-scale H_2 photoproduction requires reaching comparable efficiencies which are not yet available at the moment [3,34].

In order to achieve higher efficiency of photosynthetic H_2 production, several strategies could be employed. S-deprivation as a model approach allowed to determine several important pre-conditions for the continued H_2 production in Chlamydomonas [21]. These conditions are interdependent and could be listed as the following: (i) decrease of the PSII O_2 evolution activity and increase in the cell's respiration rate; (ii) establishing of the anoxic conditions in the cells; and (iii) establishing of the over-reduced conditions in the chloroplast [25,35–37]. It is possible to achieve these conditions by simply tuning the electron transfer in the thylakoid membrane through the adjustment of the PSII and PSI activity. As was shown by us the imbalance of the PSI/PSII ratio which creates a bottleneck for the PSII mediated electron flow by the lower PSI content in the C3 mutant in Chlamydomonas creates such conditions. This mutant was able to photoproduce H_2 continuously for more than 6 weeks [37] without any additional manipulations in a single-stage process.

Potentially, tuning of the inter photosystem electron transfer could allow sustainable and efficient H_2 production also in the wild type (WT) Chlamydomonas. One possible crucial point in the electron transfer chain for such regulation is Cyt b_6f complex [38,39]. In this study, we used dibromo-6-

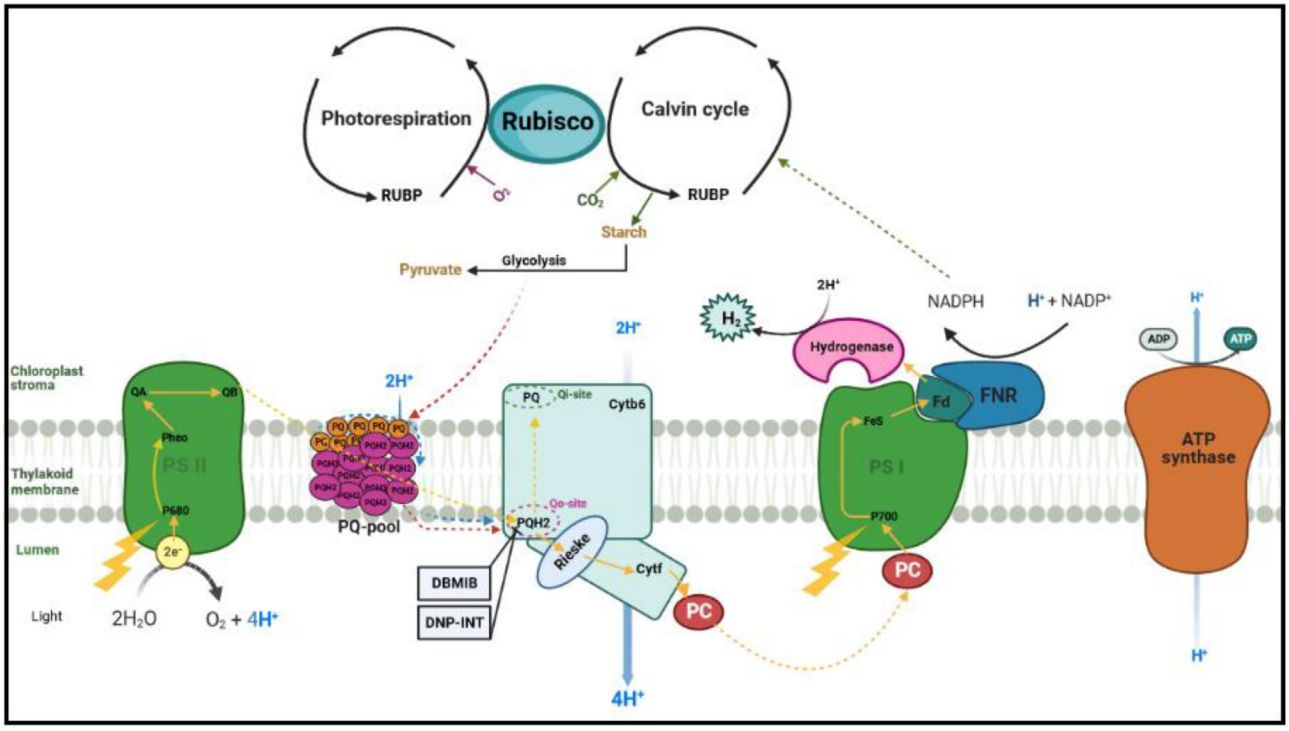

Fig. 1 – H_2 photoproduction pathways in green microalgae and the effect of DBMIB-treatment. Yellow arrows indicate the direct pathway, during which electrons evolving from water splitting in PSII are transferred towards Fd and then reach HydA, to be consumed during H_2 production. Indirect pathway is shown by red arrows and indicates electrons delivered from starch degradation to the PQ-pool. The presence of the small concentrations of DBMIB or DNP-INT, by blocking some available Qo-sites results in gradual increase of the reduction level of the PQ-pool, which is proved to be the key factor for promotion of H_2 production in our study. (For interpretation of the references to color in this figure legend, the reader is referred to the Web version of this article.)

isopropyl-3-methyl-1,4-benzoquinone (DBMIB) inhibitor which, at effective concentration (>10 μM), is known to block the PETC entirely and thus, fully inhibit the H_2 production [40,41]. Here we employ sub-optimal concentrations of DBMIB, in order to induce a controlled increase in reduction level of the PQ-pool and subsequently induce only a partial inhibition of PETC which will be most favourable for the H_2 production. Similar results were obtained with another inhibitor at the Cyt b_6f complex, 2,4-dinitrophenylether of iodonitrothymol (DNP-INT).

Materials and methods

Strains and growth conditions

Chlamydomonas reinhardtii wild-type CC-5325 strain, obtained from the Chlamydomonas Resource Center (http://www.chlamycollection.org), was maintained in plates with standard solid Tris acetate phosphate (TAP) medium [42] containing 1.5% agar. The pre-cultures were grown in liquid TAP medium in 300 ml conical glass flasks. After reaching a concentration of ~20 μg Chl/ml (corresponding to 6×10^6 cells/ml), indicated concentrations of DBMIB (from 1 mM stock solution in ethanol), were added to the culture which was then immediately transferred into the sealed bio-reactors (air-tight flasks, 300 ml culture with 20 ml gas headspace) and incubated at 25 °C under the white light of 60 μE m^{-2} s^{-1} intensity, as batch cultures, for the long-term experiments. Daily H_2 measurement from the head space was performed for 30 days.

For experiments with DNP-INT inhibitor, similar growth conditions were used. WT culture C-5325 at a Chl concentration of ~20 μg/ml was subjected to 3 different concentrations (0.6, 3.5 and 5 μM) of the inhibitor. Daily H_2 measurement from the head space was performed for 15 days.

Measuring $P700^+$ absorption changes

Kinetics of the P700 oxidation were measured with the PAM101/102 fluorometer equipped with the ED-P700DW unit (Heinz Walz GmbH, Germany) to monitor absorption changes at 810 nm using 870 nm as a reference wavelength. Actinic light was provided by PAM102 unit at 650 nm. Cell cultures at a concentration of 20 μg Chl/ml were dark adapted for 5 min before the measurements. Zero absorption (absence of $P700^+$) was measured in the presence of 5 mM ascorbate without application of the actinic light. Maximum absorption (fully oxidized P700, $P700^+$) was measured under illumination in the

presence of 10 μM DBMIB and 2 mM ferricyanide. Different concentrations of DBMIB were added from the stock solution before the measurements.

Characterization of the H_2 productivity of the cultures

H_2 and O_2 gas quantifications from the headspace of bioreactors were performed as described previously [35–37]. For the 3-(3,4-dichlorophenyl)-1,1-dimethylurea (DCMU) test, in the days 6, 9 and 22 after DBMIB-treatment, H_2 producing cultures were anaerobically aliquoted into 6 small sealed vials, in 3 of which 20 μM of DCMU was added. After 3 h of light incubation of all the vials, H_2 production rate was measured in the presence and absence of DCMU.

Chl content, flash-induced fluorescence and thermoluminescence measurements were performed according to published methods previously [35–37]. Quantifications of PSII and PSI were done by electron paramagnetic resonance (EPR) measurements with Bruker BioSpin EMX-micro spectrometer equipped with EMX-Premium bridge and an ER4119HS resonator as described previously [36,37,43]. The only modification was that the full oxidation of the $P700^+$ in cells treated with DBMIB was achieved in the presence of 17 mM ferricyanide and under illumination. Respiration and O_2 evolution rates in control or H_2 producing culture cells were measured at Chl concentration of 20 μg/ml at 25 °C with a Clark-type electrode after 3 min dark-adaptation. It was measured in the dark for 2 min followed by 3 min measurement under saturated white light.

Determination of the starch content

The starch content in cells at different time intervals after DBMIB treatment was estimated by a starch-specific enzymatic method [44]. Briefly, 10 ml aliquots of culture were harvested and centrifuged at 2450×*g* for 10 min. Resulted pellets were collected by 500 μl lysis buffer (50 mM Tris-HCl (pH = 8) and 1% Triton X-10) and after addition of 300 μl glass beads (0.7 mm), cell disintegration was performed using beadbeater (Benchmark Scientific D2400-E, USA) with 3 cycles of 30 s at 2200×*g*. Resulted cell lysates then were used for the quantification of reduced sugars through the dinitrosalicylic acid color reaction, according the previously published method [45]. The concentration of starch was estimated through a calibration curve, created by Sigma-pure potato starch digested with α-amylase.

Results

Inhibition of the PSI-driven electron transport by DBMIB treatment

Partial inhibition of the photosynthetic electron transport in Chlamydomonas cells was studied with the addition of different concentrations of DBMIB. DBMIB is a well-known inhibitor which is blocking the plastoquinole binding at the Q_o-site of the Cyt b_6f complex at the effective concentration of 10 μM [46]. The effect of the DBMIB inhibition was measured by oxidation of P700, the primary donor in PSI (Fig. 2). Upon illumination, oxidation of the P700 could be observed by monitoring the absorption changes in the far-red region [47]. In the presence of 10 mM DBMIB and 2 mM ferricyanide, the maximal oxidation level of P700 was established after ~1.2 s (Fig. 2A, red trace) since all reduction from the PSII activity was blocked by DBMIB. The absence of the $P700^+$ signal, i.e. no oxidation was determined in the dark and the presence of 5 mM of ascorbate (black trace). The addition of different concentrations of DBMIB established different steady-state levels of $P700^+$ which indicate different partial inhibition of the PETC (Fig. 2A). Inhibitory effect of DBMIB was not linear (Fig. 2B), however, we could estimate that 25%–75% inhibition of the electron transport to PSI was achieved by addition of DBMIB in the range of 0.04–5 μM concentration. Thus, different concentrations of DBMIB from this range were used in the investigation of their possible effect on the H_2 production in Chlamydomonas cells.

DBMIB induced long-term H_2 production in Chlamydomonas cells

Our next step was to find out if the addition of DBMIB in the concentration range which partially inhibited the PSI reduction have any effect on the H_2 production. The results are shown in Fig. 3. In the control culture incubated in closed bioreactors without any additions we observed no detectable H_2 production for more than two weeks. During the third week, just an insignificant amount of the H_2 release was detected (Fig. 3A, black trace). The addition of DBMIB initiated considerable H_2 production, which was concentration dependent. At very low concentrations, the H_2 production started after just a few days: at 40 nmol on the sixth day and at 200 nmol on the fifth day (pink and dark green traces). The production continued reaching 25 and 33 ml H_2/L of culture after 30 days of incubation respectively. The highest H_2 production was achieved in the presence of 3.5 μM DBMIB, which started almost immediately and could be sustained for 30 days, reaching the total amount of ~68 ml H_2/L of culture (Fig. 3A, blue trace). At higher concentrations of DBMIB, the H_2 production was again delayed and decreased, Fig. 3A (see red, light green and dark blue traces for concentrations of 5, 7.5 and 10 μmol of DBMIB).

Interestingly, the H_2 production in the presence of DBMIB not showed expected saturation behavior. A typical example can be observed at the optimal concentration of 3.5 μmol. The H_2 production started on the second day and four distinguishable outbursts of the H_2 production rate were observed during 30 days of anaerobic cultivation. The first, smallest peak was observed on the third day and followed by the largest peak on the sixth day (Fig. 3B). This maximum peak of H_2 production rate was followed by two smaller peaks, appeared at the days 9 and 22 (Fig. 3B). The peaks half-width was about 2–3 days. It should be noted that a minimum H_2 production rate (about 1 ml per L of culture per day) was maintained in between (Fig. 3B). This peculiar behavior of the H_2 production under DBMIB inhibition in Chlamydomonas cells was reproducible and this experiment was replicated in different cultures. However, it should be mentioned that the number of the H_2 production peaks and their position were very much dependent on the DBMIB concentration (not shown).

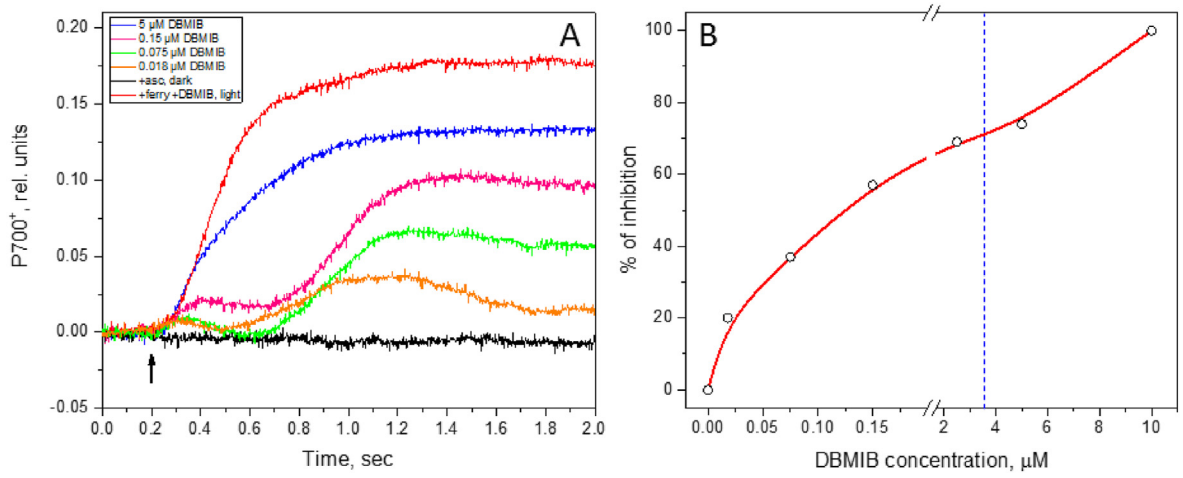

Fig. 2 – Light-induced $P700^+$ absorbance changes in cells of Chlamydomonas in the presence of different concentrations of DBMIB. A, Kinetics of P700 oxidation measured in the dark and the presence of 5 mM ascorbate (black) or under illumination in the presence of 18 nM (orange), 75 nM (green), 150 nM (pink), 5 μM (blue) and 10 μM DBMIB (red trace). The last red trace was measured also in the presence of 2 mM ferricyanide. The arrow indicates the onset of illumination. B, DBMIB concentration dependence of the steady state level of $P700^+$ achieved after 1.2 s of illumination. (For interpretation of the references to color in this figure legend, the reader is referred to the Web version of this article.)

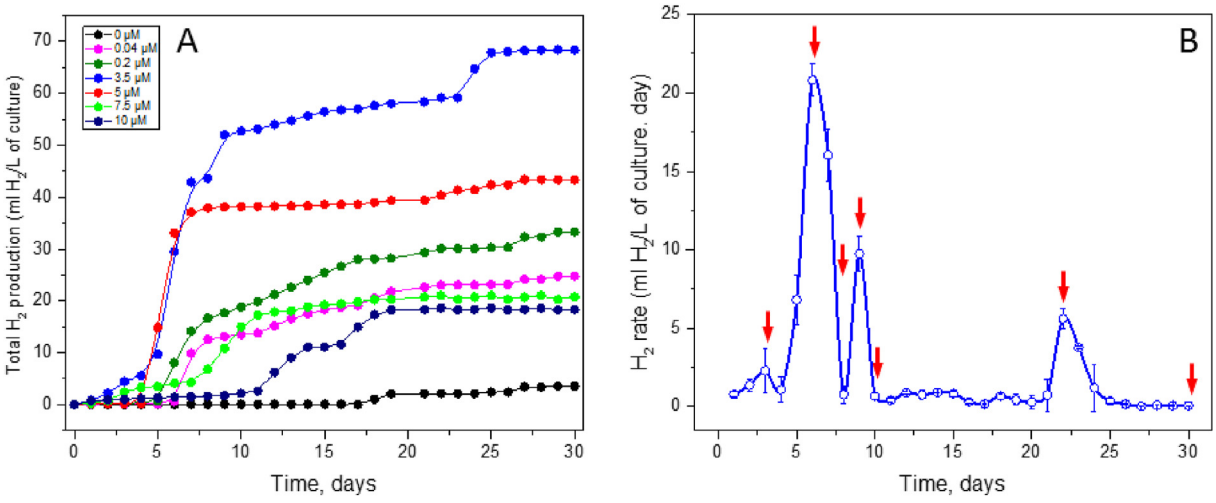

Fig. 3 – Long-term H_2 production by WT cells of Chlamydomonas, under the standard growth condition, induced by DBMIB addition. A, Total H_2 production (ml H_2 per liter of culture) in the presence of different concentrations of DBMIB. B, H_2 production rate by Chlamydomonas cells exposed to 3,5 μm DBMIB, an optimal concentration for the H_2 production. The red arrows indicate time points for cell harvesting to use the next experiments. (For interpretation of the references to color in this figure legend, the reader is referred to the Web version of this article.)

Effect of the low concentration of DBMIB on the acceptor side of PSII

In order to investigate the mechanism behind the appearance of these surges in the H_2 production rate, the cells were harvested at several different time points (shown by red arrows in Fig. 3B) for further functional analysis. While in the presence of 3.5 μM of DBMIB about 70% of the electron flow through PSI is inhibited (Fig. 2B), a similar effect was observed on the electron flow through PSII. We used flash-induced fluorescence decay measurements which are very informative on the acceptor side reactions in PSII [48–50] and were used in the characterization of H_2-producing Chlamydomonas cells before [36]. In the control cells, fluorescence decay kinetics was indicative of the fast forward electron transfer from Q_A^- (Fig. 4A, open circles) which constituted more than 85% of the kinetics (Table 1). The addition of 20 μM of DCMU effectively blocked forward electron transfer and the fluorescence decay was much slower and reflected recombination between Q_A^- and the S_2 state of the water oxidizing complex (Fig. 4A, open squares, Table 1). Noticeably, fluorescence decay measured immediately after DBMIB addition (3.5 μM) indicated only a partial inhibition of the forward electron transfer (Fig. 4A, open triangles). 53% of the fast decay phase of 646 μsec is attributed to the Q_A^- to Q_B electron transfer

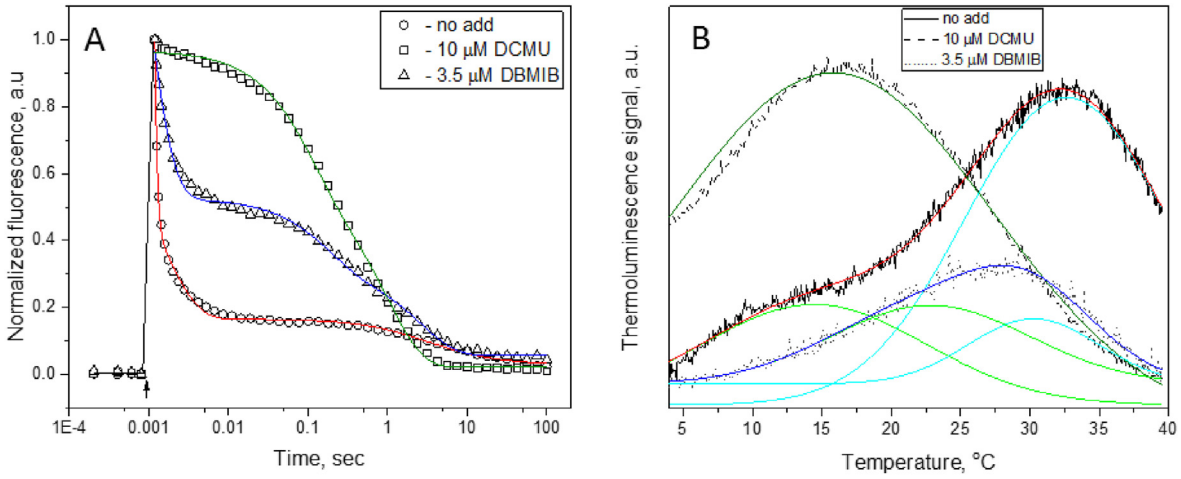

Fig. 4 – A, The flash-induced fluorescence decay traces from Chlamydomonas cells in the absence of any additions (circles), the presence of 10 μM DCMU (squares) or 3.5 μM DBMIB (triangles). Each trace represents the average of measurements in three independent samples. The lines represent exponential decay fitting (see Table 1) and the arrows indicate the position where the light flash was applied. B, Thermoluminescence curves from Chlamydomonas cells in the absence of any additions (solid black line), in the presence of 10 μM DCMU (dashed black line) or 3.5 μM DBMIB (dotted black line). Each curve represents the average of measurements in three independent samples. Green and blue lines represent Gaussian deconvolution of contributions from the Q- and B-bands respectively. (For interpretation of the references to color in this figure legend, the reader is referred to the Web version of this article.)

Table 1 – Half-times and amplitudes of the flash-induced variable fluorescence decay kinetics in Chlamydomonas cells shown in Fig. 4A. The decays were analyzed the exponential decay components as described in Ref. [36].

Sample	$t_{½,1}$, msec	$Ampl_1$, %	$t_{½,2}$, msec	$Ampl_2$, %	$t_{½,2}$, msec	$Ampl_2$, %
control (no add.)	0.084 ± 0.005	59 ± 6	1.5 ± 0.1	27 ± 5	3239 ± 486	14 ± 4
3.5 μM DBMIB	0.646 ± 0.039	53 ± 3	174 ± 28	21 ± 2	2647 ± 347	26 ± 2
10 μM DCMU	–	–	101 ± 68	45 ± 2	1019 ± 68	55 ± 2

while the middle phase (21%, 174 ms) could contain a fraction of decay that corresponds to Q_A^- to the Q_B which has to be bound first (Table 1) [48–50]. Thus, more than 50% of the electron transfer from PSII (from Q_A^-) was still active in the presence of 3.5 μM of DBMIB.

Similar results were obtained with thermoluminescence measurements (Fig. 4B). Two peaks were observed: at 33 °C and 14 °C (solid line). The dominating 33 °C peak corresponds to the B-band of the Q_B^--S_2 state recombination and reflects an active acceptor side [36,51,52]. The small shoulder at 14 °C (35% of the total intensity) represents the Q-band of the Q_A^--S_2 state recombination and becomes the only remaining at 16 °C after the addition of DCMU (dashed line, Fig. 4B).

In the presence of 3.5 μM of DBMIB a few changes were observed. First, the overall intensity decreased significantly due to the quenching which is a general effect of the quinones on the luminescence from PSII. Second, the B- and Q-bands become closer to each other (30 °C and 23 °C, respectively) and third, relatively higher intensity of the Q-band shoulder which together indicate the more reduced but still active state of the acceptor side of PSII (Fig. 4B, dotted line) [51].

PSII analysis of the DBMIB effect during H_2 production

The long-term incubation of Chlamydomonas cells with partially inhibited PETC in the presence of DBMIB resulted in the H_2 production as shown in Fig. 3. Table 2 shows that in the course of this process the total amount of chlorophyll (Chl) in the culture increased from 20 to 58 μg/ml during first 9 days and then decreased to 15 μg/ml on day 30. This indicates that cells were still growing in the first 9 days albeit at a lower rate than at the normal conditions. The Chl *a*/*b* ratio was also gradually decreasing from 2.27 to 1.11 at the same time, indicating changes in the antenna composition of PSII, mainly as decrease of the Chl *b* containing antenna complexes such as LHCII. In addition, the F_V/F_0 ratio which indicates the quantum photochemical yield of PSII was also decreasing from 0.71 to less than 0.1 during this period of 30 days with

Table 2 – Chl and fluorescence characteristics of Chlamydomonas cells during incubation for 30 days under the H_2 producing conditions in sealed bioreactors in the presence of 3.5 μM DBMIB.

Sample	Total Chl (μg/ml)	Chl *a*/*b*	F_V/F_M
day 0	20.0	2.27	0.71
day 3	32.2	2.21	0.47
day 6	36.2	2.19	0.41
day 8	44.8	2.00	0.51
day 9	58.0	2.03	0.45
day 10	50.2	1.71	0.28
day 22	27.2	1.68	0.55
day 30	15.5	1.11	0.09

exception of two time points at days 8 and 22 when it bounced back to 0.51 and 0.55 respectively (Table 2). This reflects changes in the F_0 and F_M values (Fig. 5A). The F_0 value slightly increased from 0.47 to 0.57 in the first 3 days of incubation in closed bioreactors and then started to decrease reaching a very low level of 0.15 at day 10 and then again increased to 0.20 during next 20 days. This increase could be considered as significant if the decrease of the total amount of Chl during the same time is considered (Table 2). The F_M value was constantly decreased from 1.3 to 0.2 during 30 days of incubation with one exception at day 22 (0.35, Fig. 5A).

The decrease in the F_V/F_0 ratio was accompanied with changes in the flash-induced variable fluorescence decay kinetics (Fig. 5A). The starting sample (showed more than 55% of the fast decay phases indicating partial forward electron flow from in the presence of 3.5 of DBMIB (Fig. 4A and Table 1). These kinetics didn't significantly change during next 9 days (Fig. 5A, SI Fig. 1, black traces). These kinetics were different from those measured in the presence of DCMU, where electron transfer from Q_A^- was completely blocked, although the kinetics in the presence of DBMIB become slower if compared samples from day 0 to day 9 (red traces, SI Fig. 1). Since day 10 there was no difference in the kinetics measured either in the presence or absence of DCMU, indicating completely blocked acceptor side of PSII. One exception was day 22 where some difference was observed reflecting partial reactivation of the electron transport from PSII centers. At day 30 no variable fluorescence was observed under any conditions (SI Fig. 1).

Similar changes were observed with thermoluminescence measurements (Fig. 5B). The prevailing B-band was observed during 9 days of incubation, although its intensity was decreasing after day 3 when it was at its maximum. Interestingly, it was lowest at days 6 and 9, where the first and second peaks of the H_2 production were observed (Fig. 3B and 5B and SI Fig. 2). After that, the bands measured in the presence of 3.5 μM DBMIB and in the presence of 10 μM DCMU became indistinguishable – at day10 at 26 °C and day 22 at 21 °C (Fig. 4B and SI Fig. 2). At day 30 all thermoluminescence bands were absent (Fig. 5B and SI Fig. 2).

EPR characterization of PSII and PSI during H_2 production

EPR spectroscopy is a very useful tool for the estimation of the amount of photosystems under different conditions. The amount of PSII is estimated on the basis of fully induced tyrosine (Tyr) D^{ox} radical while the amount of PSI is estimated on the basis of fully induced $P700^+$ radical as described in Ref. [43]. It has been done before for Chlamydomonas cells during the H_2 production [37]. We also performed these measurements during the incubation of Chlamydomonas cells under the H_2 producing conditions in sealed bioreactors in the presence of 3.5 μM of DBMIB.

At day 0 cells show standard amounts of PSII and PSI as could be judged from the corresponding spectra (Fig. 6A). Almost equal amount of both photosystems was observed resulting in a PSII/PSI ratio of 0.84 (Fig. 6D). PSII and PSI behaved differently during 30 days of incubation. The amount of PSII decreased to less than 60% until day 8, then increased during days 9 and 10 to more than 90% and then decreased again to 59% and 40% at day 22 and day 30 respectively (Fig. 6B and C, green bars). In contrast, the amount of PSI is first decreased to 60% at day 6 and then started to increase, especially significantly during days 9 and 10 (to more than 400%), reaching 436% at day 22 and 532% at day 30 respectively (Fig. 6B and C, red bars). These changes resulted in a steady increase of the PSI/PSII ratio from day 8 to almost 11 at day 30 (Fig. 6D).

Direct vs indirect pathway in the DBMIB treated cells

To estimate the contribution of PSII in producing H_2 at each peak of the H_2 production, the DCMU test was performed [35,53–55]. DCMU is another well-known inhibitor which

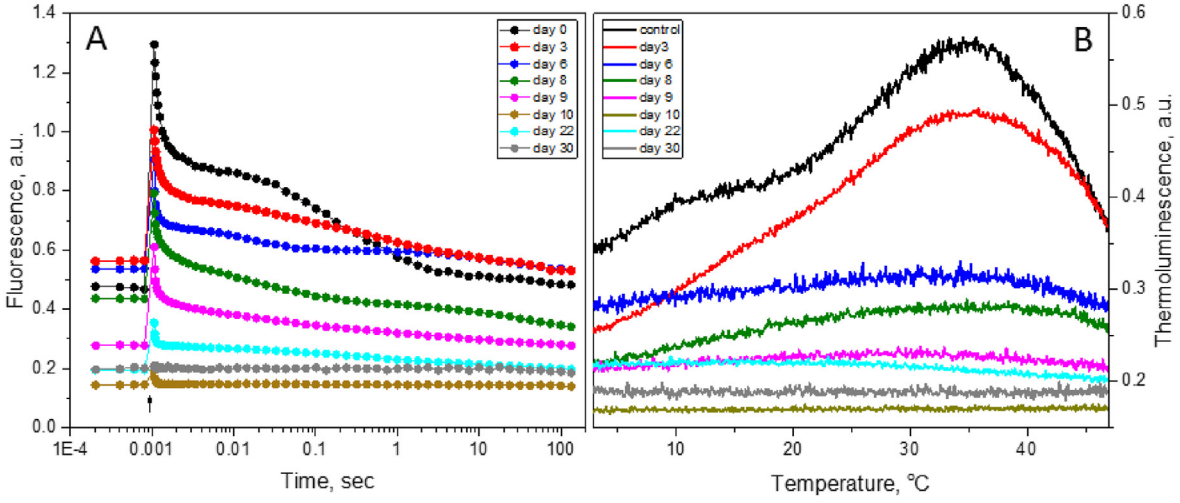

Fig. 5 – A, The flash-induced fluorescence decay traces from Chlamydomonas cells during 30 days of incubation under the H_2 producing conditions in sealed bioreactors in the presence of 3.5 μM DBMIB. Traces are normalized to the Chl concentration. Each trace represents the average of measurements in three independent samples. B, Thermoluminescence curves from Chlamydomonas cells during 30 days of incubation under the H_2 producing conditions in sealed bioreactors in the presence of 3.5 μM DBMIB. Traces are normalized to the Chl concentration. Each trace represents the average of measurements in three independent samples.

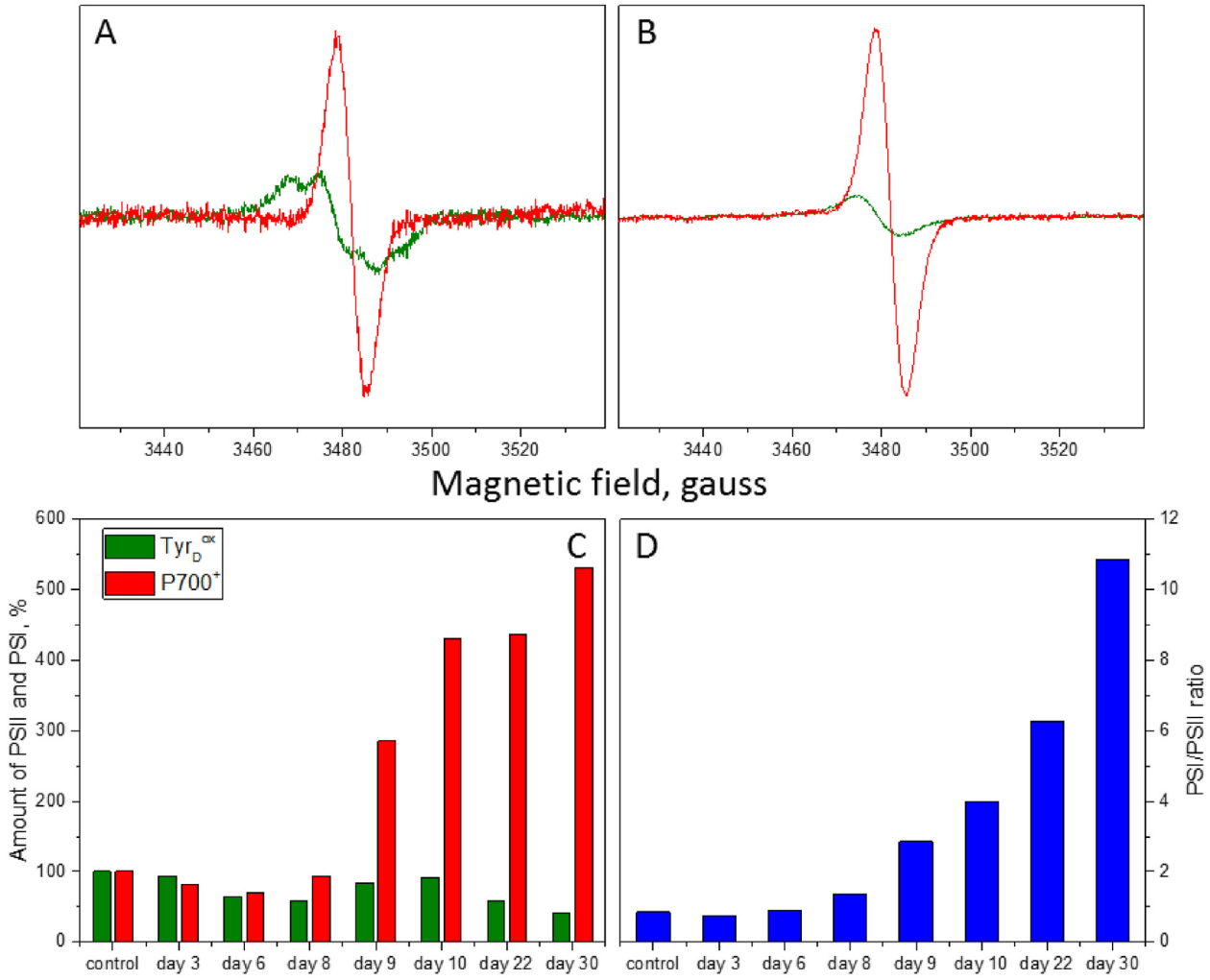

Fig. 6 – EPR measurements showing Tyr_D^{ox} (green spectrum) and $P700^+$ (red spectrum) from Chlamydomonas cells under the H_2 producing conditions in sealed bioreactors in the presence of 3.5 μM DBMIB in day 0 (A) and day 9 (B). C, Changes in the amount of PSII (measured as Tyr_D^{ox} (green bars) and PSI (measured as $P700^+$ (red bars) under the H_2 producing conditions for 30 days in the presence of 3.5 μM DBMIB. The amount of both photosystems at day 0 were taken as 100%. D, Changes in the PSI/PSII ratio under the H_2 producing conditions for 30 days in the presence of 3.5 μM DBMIB. (For interpretation of the references to color in this figure legend, the reader is referred to the Web version of this article.)

effectively blocks PSII electron transport at the Q_B-site. According to our results (Fig. 7A), the addition of DCMU inhibited more than 72% of H_2 production at the first peak on day 6. In contrast, at the second and third peaks on day 9 and 22, only around 6% and 19% of the H_2 production respectively was suppressed by PSII-inhibition. This indicates that on day 6, more than 70% of produced H_2 came from the direct pathway, whereas produced H_2 in the second and third peaks was almost entirely PSII-independent, mediated by the indirect pathway (Fig. 7A).

Taking into account that during the indirect pathway, starch degradation is the main source of electrons for the H_2 production, we measured the level of starch accumulation at the same time points as above. We observed more than 50% decrease of the starch amount after DBMIB addition on days 6 and 9, if compared to control (Fig. 7B). This decrease is a consequence of starch degradation in the cells. However, on day 22, the starch level was detected to be even higher than in the control cells (Fig. 7B). This increase could be attributed to hyper-accumulation of starch in response to the nutrient starvation of Chlamydomonas cells, after being in batch culture for more than 3 weeks [56,57].

In order to obtain more insight about the circumstances of the H_2 production outbursts, we also measured the net O_2 evolution rate in day 3 and 6 after the DBMIB addition. The net O_2 evolution rate is considered as the difference between the rates of gross O_2 evolution and O_2 uptake (respiration) under illumination and was measured in μmol O_2/ml of culture × min. The average net rate of O_2 evolution in the control cells was 5.6 μmol O_2. This net rate was decreased to 1.7 μmol O_2 on day 3 and to −5.1 μmol O_2 on day 6 after the DBMIB treatment (not shown). Thus, during the peak of H_2 production, respiration completely overtook the O_2 evolution by PSII in Chlamydomonas cells.

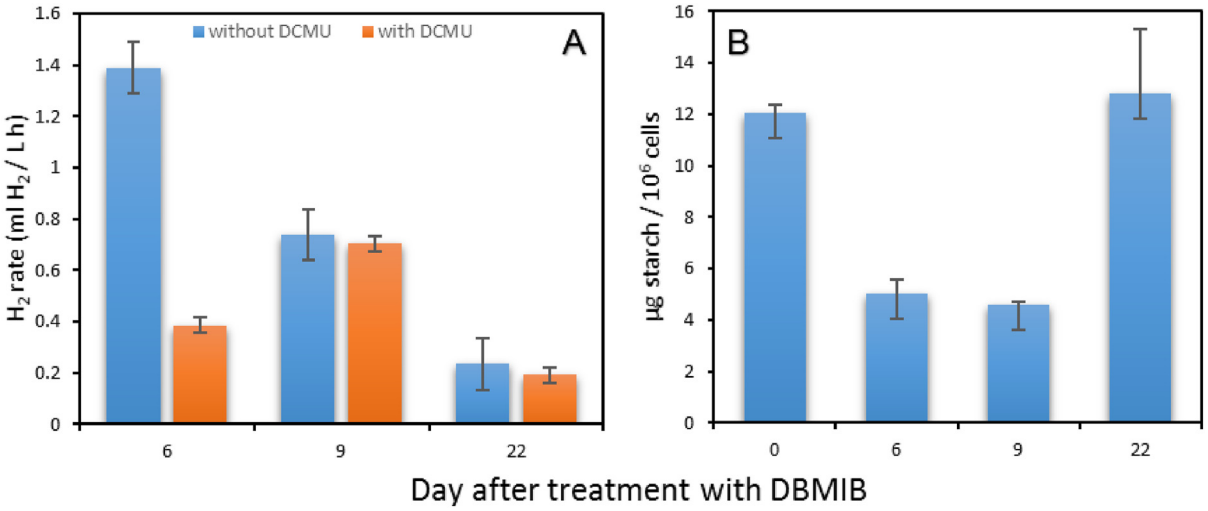

Fig. 7 – A, H_2 production rate of DBMIB-treated cultures in the presence vs in the absence of DCMU inhibitor (20 μM). B, estimated starch content of DBMIB-treated cells, measured under H2-producing condition, in 3 different time points corresponding to the peaks of H_2 production rate.

DNP-INT-induced long-term H_2 production in Chlamydomonas cells

There is another electron transport inhibitor which also acts at the Q_o-site of Cyt b_6f complex, DNP-INT. Addition of 0.6 and 3.5 μM of DNP-INT resulted in H_2 production for at least 15 days (Fig. 8). The best result was achieved in the presence of 0.6 μM of DNP-INT with the maximal rate of ~4 ml of H_2 per L of culture per day achieved on the day 7 of incubation (inset in Fig. 8), which was more than 5 times lower than highest rate achieved in the presence of DBMIB (Fig. 3B). There could be two reasons for this difference. Firstly, these inhibitors, although having the same binding side in the Cyt b_6f complex, have different chemical nature and correspondingly could have different life-time inside of the cell environment. Secondly, it has been recently reported that DNP-INT is not able to completely block electron transfer to PSI but rather effectively slows down this reaction [58]. These could lead to different rates of the inter-photosystem electron transfer and correspondingly, to the different mode of the H_2 photoproduction in the presence of DNP-INT.

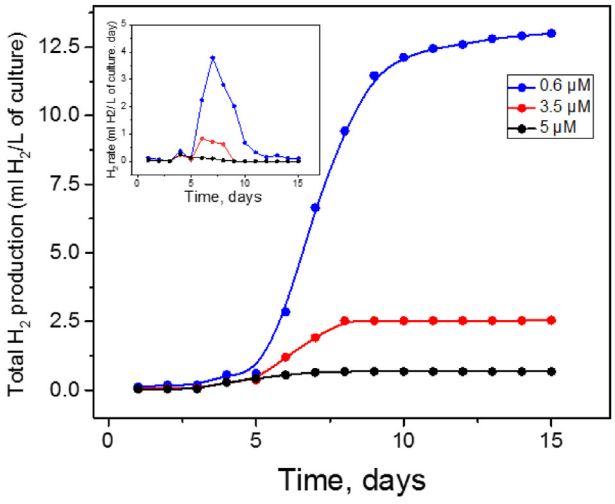

Fig. 8 – Long-term H_2 production by WT cells of Chlamydomonas, under the standard growth condition, induced by DNP-INT addition at concentration of 0.6 μM (blue), 3.5 μM (red) and 5 μM (black). Inset shows the H_2 production rates. (For interpretation of the references to color in this figure legend, the reader is referred to the Web version of this article.)

Discussion

Sustainable H_2 production in green microalgae

To achieve a commercially viable green H_2 production, the ideal solution would be to achieve (i) an efficient, (ii) sustainable H_2-photoproduction (iii) in a simple scalable model using WT strains of green microalgae such as Chlamydomonas. Use of genetically modified strains with manipulated PETC, or enhanced tolerance of HydA to O_2, although practical, could also be questionable for large scale applications. According to a recent study, utilization of the GMOs for biofuel production is still a big concern for experts and stakeholders [59].

In the current study we utilized these solutions to achieve H_2 production in WT strain CC-5325 of Chlamydomonas for 30 days, in a single-stage mode. Our main approach to achieve this was to re-tune the electron flow to final acceptors (Fig. 1). Regulation of the photosynthetic electron flow is already a quite complex process in Chlamydomonas [40,60,61] and additional de-regulation should not add more complications for sustaining process on the long run without sacrificing the cell viability. It should lead to the restricting of the PSII activity and increase of the reduction level of the PQ-pool. Under such conditions the prolonged H_2 production is expected [25,35,36]. In our previous study we achieved this by decreasing the amount of PSI, thus hindering the electron flow and creating the "bottleneck" at the Cyt b_6f complex [37]. In this study, we

achieved this by addition of the small concentrations of Cyt b_6f inhibitors to the media culture of WT Chlamydomonas.

It is known that at effective concentrations of DBMIB (>10 μM) the electron transfer to PSI is halted and H_2 production in S-deprived cultures of Chlamydomonas is almost completely inhibited [53–55]. We anticipated that after addition of small concentrations of DBMIB, some of the available Q_o-sites in $Cytb_6f$ would be occupied, leading to the decrease of the electron flow to PSI, increase of the reduction level of the PQ-pool and subsequently partial quenching of electron transport from PSII. The down-regulation of PSII activity will establish the microoxic condition which will, in turn, activate HydA and end up in prolonged H_2 evolution.

Our findings confirmed the principle of these assumptions, when different levels of PSI oxidation, PQ-pool reduction and PSII activity were detected after the DBMIB treatment (see below). However, the outcome of this treatment was much more complicated. We observed that there was no linear correlation between the DBMIB concentration and the level of PSI oxidation (Fig. 2B). Externally induced changes in the PETC, involved internal interactions within the cells which were followed by intrinsic regulatory mechanisms to maintain a partially operational PETC and to retain its integrity for at least 30 days (Fig. 3).

This duration of H_2 productivity in WT strain is quite unprecedented and ended up in a high total H_2 yield. This production period in DBMIB treated WT, is comparable with what was previously reported for the C3 mutant [37]. However, the total produced H_2 and the max H_2 production rate, obtained in this study, were respectively 1.3 times and 6.7 times higher than what was shown in the C3 mutant (Krishna et al., 2019). 3.5 μM DBMIB turned out to be the optimal concentration for this sustained H_2 photoproduction (Fig. 3A). However, the nature of this photoproduction was not steady, with several surges of H_2 evolution with high rates present (Fig. 3B), indicating complex intracellular reactions.

Suggested mechanism for H_2 production in DBMIB-treated cells

The H_2 production rate in the presence of 3.5 μM DBMIB was not constant during the whole 30 days period of cells incubation. The maximum rate was obtained 6 days after the addition. Comparing the results of fluorescence decay measurements, thermoluminescence (Fig. 5) and EPR analysis (Fig. 6) with the results of DCMU test (Fig. 7A) we can conclude that on day 6, the amount of PSII is still quite high (65% of control, Fig. 6C) and these PSII centers exhibit quite active forward electron transfer (Fig. 5, SI Figs. 1 and 2). Together with similar amount of PSI (Fig. 6C), PSII mediates more than 70% of H_2 production, via the direct biophotolysis of water (yellow arrows in Fig. 1). Although reduction level of the PQ-pool was also high as also shown by the fluorescence and thermoluminescence measurements, this amount of stable and active PSII on day 6 should produce enough O_2 to suppress the HydA activity, while the maximum rate of H_2 production was ascertained on this day.

The measured net O_2 evolution rate and the starch content could explain this contradiction. Indeed, by detecting a higher rate of O_2 consumption than O_2 evolution, together with a diminished starch content (down to 50%, Fig. 7B), we can assume an up-regulated photorespiration on the day 6 after addition of DBMIB to Chlamydomonas cells. Photorespiration which arises from the oxygenase activity of Rubisco [62], is known as a wasteful process which diminishes CO_2 fixation, and thus decreases the starch content. In a recent study it was shown that the thioredoxin-mediated regulation of photorespiration takes place in response to the redox state of chloroplast [63]. Accordingly, we can propose that DBMIB addition induces up-regulation of photorespiration, when thioredoxin is reduced as a consequence of the redox state of the PQ-pool. In addition to establishment of anoxia, this process would be accompanied with down regulation of the CO_2 fixation, thus increasing the electron allocation to HydA, resulting in a high H_2 production rate during the first outburst (days 5–7, Fig. 3B). The following termination of the H_2 production, observed in the day 8, could be explained by relaxation of the electron pressure after 3 consecutive days of H_2 production at a high rate. In addition, the increased presence of O_2 due to reactivated PSII contributed to this step. Similar mechanism could be responsible for the single peak of H_2 production in the presence of DNP-INT (Fig. 8). This presumption is in line with the physiological role of the H_2 production in Chlamydomonas as an energy dissipating pathway under anaerobic and/or reduced condition [64,65].

In addition, another mechanism, involving chlororespiration, catalyzed by the plastid alternative oxidase (PTOX), could lead to the DBMIB-induced microoxic conditions. Recently, it was shown that PTOX is induced in response to the reduced state of the PQ-pool and inactivated upon relief of extra electrons [66]. Our assumption is that PTOX activity is induced after 6 days of DBMIB addition, when PQ-pool is reduced enough, establishing a microoxic condition for HydA while PSII still remains quite active. Then, as a consequence of the PQ-pool being relieved of extra electrons, PTOX is inactivated, leading to a decline in H_2 production rate on day 8.

Shortly after this sharp decrease, the second peak of H_2 production appears, lasting for only one day. We propose that soon after relieving the reductive conditions by the first outburst of H_2 release (on day 8) and thus, favoring electrons redirection back to CCB cycle, the reducing conditions were recreated in the thylakoid membrane and stromal compartment. In this case the majority of electrons which were available from the starch degradation, contributes to the second outburst of the H_2 production via the indirect pathway (day 9, Figs. 5 and 6C and D), as was shown by the DCMU test (~95%, Fig. 7A).

Then, after some time (on day 10), electron flow to HydA would be outcompeted by FNR again. Nevertheless, a minimum H_2 production rate (1 ml H_2 per L culture × day) was maintained for the whole incubation period, with a third small outburst of H_2 appearing on day 22 (Fig. 3B). The last outburst was accompanied with accumulation of starch during last 11 days (Fig. 7B), when again the PSII-independent pathway turned to be in charge of H_2 production (more than 80%), while remaining PSII (~60%, Fig. 6C) were still able to deliver about the rest of 20% of electrons to HydA on day 22 (Fig. 7A).

Conclusions

The present study demonstrated that Cyt b_6f complex plays an important role in modulating the redox state of the PQ-pool and in initiation and maintaining the H_2 production in Chlamydomonas. By regulation the PETC at the Cyt b_6f complex level, other metabolic reactions in chloroplast such as photorespiration and starch accumulation can be switched on and off, placing cells between photosynthetic, H_2 producing and survival modes of metabolism. Introducing and maintaining such control mechanism in *Chlamydomonas reinhardtii* could break ground for long lasting direct and efficient H_2 photoproduction with potential for the industrial scale-up applications.

Declaration of competing interest

The authors declare that they have no known competing financial interests or personal relationships that could have appeared to influence the work reported in this paper.

Acknowledgment

Authors are grateful to the Carl Tryggers Foundation for financial support (grant CTS 19:230). Ms. Elodie Blanc is acknowledged for performing the initial experiments with DBMIB.

Appendix A. Supplementary data

Supplementary data to this article can be found online at https://doi.org/10.1016/j.ijhydene.2023.06.050.

REFERENCES

[1] Executive summary - global hydrogen review. 2021 - analysis. IEA; 2022.
[2] Chen YM. Global potential of algae-based photobiological hydrogen production. Energy Environ Sci 2022;15:2843–57.
[3] Wang Y, Yang HL, Zhang XN, Han F, Tu WF, Yang WQ. Microalgal hydrogen åroduction. Small Methods 2020;4:1900514.
[4] Torzillo G, Scoma A, Faraloni C, Giannelli L. Advances in the biotechnology of hydrogen production with the microalga Chlamydomonas reinhardtii. Crit Rev Biotechnol 2015;35:485–96.
[5] Ghirardi ML, Dubini A, Yu JP, Maness PC. Photobiological hydrogen-producing systems. Chem Soc Rev 2009;38:52–61.
[6] Magnuson A, Mamedov F, Messinger J. Toward sustainable H_2 production: linking hydrogenase with photosynthesis. Joule 2020;4:1157–9.
[7] Shevela D, Kern JF, Govindjee G, Messinger J. Solar energy conversion by photosystem II: principles and structures. Photosynth Res 2023;156:279–307.
[8] Hauska G, Schutz M, Büttner B. The cytochrome b_6f complex – composition, structure and function. In: Ort DR, Yocum CF, Heichel IF, editors. Oxygenic photosynthesis: the light reactions. Dordrecht: Springer; 1966. p. 377–98.
[9] Brettel K, Leibl W. Electron transfer in photosystem I. Biochim Biophys Acta 2001;1507:100–14.
[10] Bukhov N, Carpentier R. Alternative Photosystem I driven electron transport routes: mechanisms and functions. Photosynth Res 2004;82:17–33.
[11] Hatch MD, Slack CR. Photosynthetic CO_2-fixation pathways. Annu Rev Plant Physiol 1970;21:141–62.
[12] Tagawa K, Arnon DI, Tsujimoto HY. Role of chloroplast ferredoxin in energy conversion process of photosynthesis. Proc Natl Acad Sci USA 1963;49:567–72.
[13] Finazzi G, Rappaport F, Furia A, Fleischmann M, Rochaix JD, Zito F, et al. Involvement of state transitions in the switch between linear and cyclic electron flow in *Chlamydomonas reinhardtii*. EMBO Rep 2002;3:280–5.
[14] Benemann JR. Feasibility analysis of photobiological hydrogen production. Int J Hydrogen Energy 1997;22:979–87.
[15] Khosravitabar F. Microalgal biohydrogen photoproduction: scaling up challenges and the ways forward. J Appl Phycol 2020;32:277–89.
[16] Ramprakash B, Lindblad P, Eaton-Rye JJ, Incharoensakdi A. Current strategies and future perspectives in biological hydrogen production: a review. Renew Sustain Energy Rev 2022;168:112773.
[17] Dubini A, Ghirardi ML. Engineering photosynthetic organisms for the production of biohydrogen. Photosynth Res 2015;123:241–53.
[18] Milrad Y, Schweitzer S, Feldman Y, Yacoby I. Green algal hydrogenase activity is outcompeted by carbon fixation before inactivation by oxygen takes place. Plant Physiol 2018;177:918–26.
[19] Ghirardi ML, Seibert M. Techniques for isolation of oxygen-tolerant mutants of hydrogen-producing *Chlamydomonas reinhardtii*. Plant Physiol 1997;114:1027.
[20] Touloupakis E, Faraloni C, Silva Benavides AM, Torzillo G. Recent achievements in microalgal photobiological hydrogen production. Energies 2021;14:7170.
[21] Melis A, Zhang L, Forestier M, Ghirardi ML, Seibert M. Sustained photobiological hydrogen gas production upon reversible inactivation of oxygen evolution in the green alga *Chlamydomonas reinhardtii*. Plant Physiol 2000;122:127–36.
[22] Lari Z, Khosravitabar F. A comparative review on different trophic modes and useable carbon sources for microalgae cultivation, approaching to optimize lipid åroduction in trade scale. Syst Biosci Engin 2021:16–26.
[23] Mandotra SK, Sharma C, Srivastava N, Ahluwalia AS, Ramteke PW. Current prospects and future developments in algal bio-hydrogen production: a review. Biomass Conv Bioref.; 2021.
[24] Philipps G, Happe T, Hemschemeier A. Nitrogen deprivation results in photosynthetic hydrogen production in *Chlamydomonas reinhardtii*. Planta 2012;235:729–45.
[25] Volgusheva A, Kukarskikh G, Krendeleva T, Rubin A, Mamedov F. Hydrogen photoproduction in green algae Chlamydomonas reinhardtii under magnesium deprivation. RSC Adv 2015;5:5633–7.
[26] Batyrova KA, Tsygankov AA, Kosourov SN. Sustained hydrogen photoproduction by phosphorus-deprived *Chlamydomonas reinhardtii* cultures. Int J Hydrogen Energy 2012;37:8834–9.
[27] Surzycki R, Cournac L, Peltiert G, Rochaix JD. Potential for hydrogen production with inducible chloroplast gene expression in Chlamydomonas. Proc Natl Acad Sci USA 2007;104:17548–53.
[28] Scoma A, Krawietz D, Faraloni C, Giannelli L, Happe T, Torzillo G. Sustained H-2 production in a *Chlamydomonas reinhardtii* D1 protein mutant. J Biotechnol 2012;157:613–9.

[29] Steinbeck J, Nikolova D, Weingarten R, Johnson X, Richaud P, Peltier G, et al. Deletion of proton gradient regulation 5 (PGR5) and PGR5-like 1 (PGRL1) proteins promote sustainable light-driven hydrogen production in *Chlamydomonas reinhardtii* due to increased PSII activity under sulfur deprivation. Front Plant Sci 2015;6.
[30] Liu P, Ye DM, Chen M, Zhang J, Huang XH, Shen LL, et al. Scaling-up and proteomic analysis reveals photosynthetic and metabolic insights toward prolonged H_2 photoproduction in Chlamydomonas hpm91 mutant lacking proton gradient regulation 5 (PGR5). Photosynth Res 2022;154:397–411.
[31] Khosravitabar F, Hippler M. A new approach for improving microalgal biohydrogen photoproduction based on safe and fast oxygen consumption. Int J Hydrogen Energy 2019;44:17835–44.
[32] Paramesh K, Chandrasekhar T. Improvement of photobiological hydrogen production in *Chlorococcum minutum* using various oxygen scavengers. Int J Hydrogen Energy 2020;45:7641–6.
[33] Elman T, Hoai Ho TT, Milrad Y, Hippler M, Yacoby I. Enhanced chloroplast-mitochondria crosstalk promotes ambient algal H_2 production. Cell Rep Physic Scie 2022;3:100828.
[34] Li SN, Li FH, Zhu X, Liao Q, Chang JS, Ho SH. Biohydrogen production from microalgae for environmental sustainability. Chemosphere 2022:291.
[35] Volgusheva A, Styring S, Mamedov F. Increased photosystem II stability promotes H_2 production in sulfur-deprived *Chlamydomonas reinhardtii*. Proc Natl Acad Sci USA 2013;110:7223–8.
[36] Volgusheva A, Kruse O, Styring S, Mamedov F. Changes in the photosystem II complex associated with hydrogen formation in sulfur deprived *Chlamydomonas reinhardtii*. Algal Res 2016;18:296–304.
[37] Krishna PS, Styring S, Mamedov F. Photosystem ratio imbalance promotes direct sustainable H_2 production in *Chlamydomonas reinhardtii*. Green Chem 2019;21:4683–90.
[38] Zito F, Finazzi G, Joliot P, Wollman FA. Glu78, from the conserved PEWY sequence of subunit IV, has a key function in cytochrome b_6f turnover. Biochemistry 1998;37:10395–403.
[39] Baniulis D, Yamashita E, Zhang H, Hasan SS, Cramer WA. Structure-Function of the cytochrome b_6f complex. Photochem Photobiol 2008;84:1349–58.
[40] Finazzi G, Furia A, Barbagallo RP, Forti G. State transitions, cyclic and linear electron transport and photophosphorylation in *Chlamydomonas reinhardtii*. Biochim Biophys Acta 1999;1413:117–29.
[41] Alric J, Lavergne J, Rappaport F. Redox and ATP control of photosynthetic cyclic electron flow in *Chlamydomonas reinhardtii* aerobic conditions. Biochim Biophys Acta 2010;1797:44–51.
[42] Gorman DS, Levine RP. Cytochrome f and plastocyanin: their sequence in the photosynthetic electron transport chain of *Chlamydomonas reinhardi*. Proc Natl Acad Sci USA 1965;54:1665–9.
[43] Danielsson R, Albertsson P-Å, Mamedov F, Styring S. Quantification of photosystem I and II in different parts of the thylakoid membrane from spinach. Biochim Biophys Acta 2004;1608:53–61.
[44] Miller GL. Use of dinitrosalicylic acid reagent for determination of reducing sugar. Anal Chem 1959;31:426–8.
[45] Ivanov IN, Zachleder V, Vitova M, Barbosa MJ, Bisova K. Starch production in *Chlamydomonas reinhardtii* through supraoptimal temperature in a pilot-scale photobioreactor. Cells 2021;10.
[46] Barbagallo RP, Finazzi G, Forti G. Effects of inhibitors on the activity of the cytochrome b_6f complex: evidence for the existence of two binding pockets in the lumenal site. Biochemistry 1999;38:12814–21.
[47] Schreiber U. Pulse-amplitude-modulation (PAM) fluorometry and saturation pulse method: an overview. In: Papageorgiou GC, Govindjee, editors. Chlorophyll a fluorescence: a signature of photosynthesis. Dordrecht: Springer Netherlands; 2004. p. 279–319.
[48] Vass I, Kirilovsky D, Etienne A-L. UV-B radiation-induced donor- and acceptor-side modifications of photosystem II in the cyanobacterium *Synechocystis sp*. PCC 6803. Biochemistry 1999;38:12786–94.
[49] Mamedov F, Stefansson H, Albertsson P-Å, Styring S. Photosystem II in different parts of the thylakoid membrane: a functional comparison between different domains. Biochemistry 2000;39:10478–86.
[50] Roose JL, Frankel LK, Bricker TM. Documentation of significant electron transport defects on the reducing side of photosystem ii upon removal of the Psbp and Psbq extrinsic proteins. Biochemistry 2010;49:36–41.
[51] Vass I. The history of photosynthetic thermoluminescence. Photosynth Res 2003;76:303–18.
[52] Ducruet J-M, Peeva V, Havaux M. Chlorophyll thermofluorescence and thermoluminescence as complementary tools for the study of temperature stress in plants. Photosynth Res 2007;93:159–71.
[53] Antal TK, Volgusheva AA, Kukarskih GP, Krendeleva TE, Rubin AB. Relationships between H-2 photoproduction and different electron transport pathways in sulfur-deprived *Chlamydomonas reinhardtii*. Int J Hydrogen Energy 2009;34:9087–94.
[54] Kosourov S, Seibert M, Ghirardi ML. Effects of extracellular pH on the metabolic pathways in sulfur-deprived, H_2-producing *Chlamydomonas reinhardtii* cultures. Plant Cell Physiol 2003;44:146–55.
[55] Krishna PS, Morello G, Mamedov F. Characterization of the transient fluorescence wave phenomenon that occurs during H_2 production in *Chlamydomonas reinhardtii*. J Experim Botany 2019;70:6321–36.
[56] Ball SG, Dirick L, Decq A, Martiat JC, Matagne RF. Physiology of starch storage in the monocellular alga *Chlamydomonas reinhardtii*. Plant Sci 1990;66:1–9.
[57] Schulz-Raffelt M, Chochois V, Auroy P, Cuiné S, Billon E, Dauvillée D, et al. Hyper-accumulation of starch and oil in a Chlamydomonas mutant affected in a plant-specific DYRK kinase. Biotechnol Biofuels 2016;9:55.
[58] Fitzpatrick D, Aro EM, Tiwari A. A commonly used photosynthetic inhibitor fails to block electron flow to photosystem i in intact systems. Front Plant Sci 2020;11.
[59] Villarreal JV, Burgues C, Rosch C. Acceptability of genetically engineered algae biofuels in Europe: opinions of experts and stakeholders. Biotechnol Biofuels 2020;13.
[60] Lucker B, Kramer DM. Regulation of cyclic electron flow in *Chlamydomonas reinhardtii* under fluctuating carbon availability. Photosynth Res 2013;117:449–59.
[61] Minagawa J, Tokutsu R. Dynamic regulation of photosynthesis in *Chlamydomonas reinhardtii*. Plant J 2015;82:413–28.
[62] Bathellier C, Yu LJ, Farquhar GD, Coote ML, Lorimer GH, Tcherkez G. Ribulose 1,5-bisphosphate carboxylase/oxygenase activates O_2 by electron transfer. Proc Natl Acad Sci USA 2020;117:24234–42.
[63] da Fonseca-Pereira P, Souza PVL, Fernie AR, Timm S, Daloso DM, Araújo WL. Thioredoxin-mediated regulation of

photorespiration and central metabolism. J Experim Botany 2021;72:5987–6002.
[64] Hemschemeier A, Fouchard S, Cournac L, Peltier G, Happe T. Hydrogen production by *Chlamydomonas reinhardtii*: an elaborate interplay of electron sources and sinks. Planta 2008;227:397–407.
[65] Hemschemeier A, Happe T. Alternative photosynthetic electron transport pathways during anaerobiosis in the green alga Chlamydomonas reinhardtii. Biochim Biophys Acta 2011;1807:919–26.
[66] Saroussi S, Redekop P, Karns DAJ, Thomas DC, Wittkopp TM, Posewitz MC, et al. Restricting electron flow at cytochrome b_6f when downstream electron acceptors are severely limited. Plant Physiol 2023;192:789–804.